Supporting Information

Experimental

Crystal structure data

4CC-y: Yellow plate recrystallized with acetone. $C_{13}H_9Cl_2NO$, Mw = 266.12, monoclinic, a = 6.140(5), b = 6.848(6), c = 27.39(2) Å, β = 95.26(2)°, V = 1146.6(16) Å^3, D_{calcd} = 1.541 g/cm^3, T = 93 K, space group $I2/c$ (#15), Z = 4, μ(Mo-Kα) = 5.45 cm^{-1}, F(000) = 544, 6509 reflections measured and 2453 unique ($2\theta_{max}$=54.9°, R_{int} = 0.0462) which were used in all calculations. Goodness-of-fit on F^2 = 1.113, R = 0.0447, R_w = 0.1002.

4CC-o: Orange plate recrystallized with acetone. $C_{13}H_9Cl_2NO$, Mw = 266.12, monoclinic, a = 10.004(6), b = 4.688(3), c = 11.919(7) Å, β = 93.2393(10)°, V = 558.1(6) Å^3, D_{calcd} = 1.584 g/cm^3, T = 93 K, space group $P2_1/c$ (#14), Z = 2, μ(Mo-Kα) = 5.60 cm^{-1}, F(000) = 272, 6549 reflections measured and 1275 unique ($2\theta_{max}$=55.0°, R_{int} = 0.0530) which were used in all calculations. Goodness-of-fit on F^2 = 1.265, R = 0.0504, R_w = 0.1208.

5CC-o: Orange needle recrystallized with dichloromethane and hexane. $C_{13}H_9Cl_2NO$, Mw = 266.12, monoclinic, a = 20.427(6), b = 4.5728(13), c = 12.101(4) Å, β = 92.301(5) °, V = 1129.4(6) Å^3, D_{calcd} = 1.565 g/cm^3, T = 93 K, space group $P2_1/c$ (#14), Z = 4, μ(Mo-Kα) = 5.54 cm^{-1}, F(000) = 544, 12645 reflections measured and 2578 unique ($2\theta_{max}$=55.0°, R_{int} = 0.0467) which were used in all calculations. Goodness-of-fit on F^2 = 1.072, R = 0.0333, R_w = 0.0830.

Tables and Drawing Objects

Table S1 Forms (Y: yellow, O: orange)[a] of crystals obtained when saturated solutions (25°C) was cooled down to 0°C.

Compound	4CC		5CC	
Times elapsed	1h	24h	1h	24h
Methanol	Y + O_{tr}	Y + O_{tr}	Y + O_{tr}	Y + O_{tr}
Ethanol	Y	Y	Y	Y
Pyridine	Y[b]	Y	Y[b]	Y
Acetone	Y	O	O	O
Acetonitrile	O	O	Y_{tr} + O	Y_{tr} + O
Dichloromethane	Y + O	O[c]	O	O

a) Subscript "tr" denotes trace amount. b) After 4h. c) After 12h at 4°C.

Table S2 ΔH / J mol^{-1} (peak temperature / °C) measured at heating/cooling rate of 2 K/min.

	Heating process	Cooling process	
4CC-y			
1st cycle	34.1 (156.0)	−29.3 (123.7)	
2nd cycle	30.6 (146.0)	−29.1 (124.0)	
3rd cycle	32.8 (155.0)	−30.9 (123.4)	
4CC-o			
1st cycle	35.2 (154.9)	−30.5 (122.6)	
2nd cycle	34.1 (153.7)	−30.6 (123.1)	
5CC-y			
1st cycle	33.3 (149.4)	−28.2 (131.5)	−3.6 (115.0)
2nd cycle	33.6 (149.5)	−28.1 (129.5)	−3.8 (126.5)
5CC-o			
1st cycle	34.2 (150.1)	−29.1 (130.1)	−3.7 (123.5)
2nd cycle	33.9 (149.4)	−29.0 (130.0)	−3.7 (120.6)

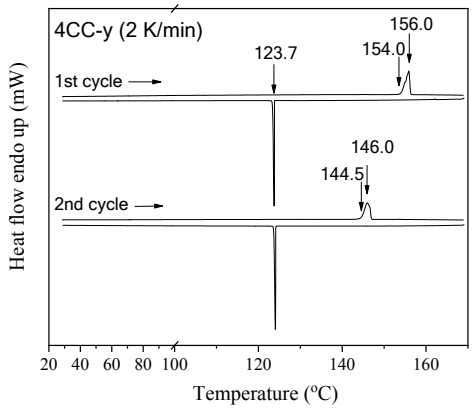
4CC-y (2 K/min)
1st cycle
2nd cycle
123.7
156.0
154.0
146.0
144.5
Heat flow endo up (mW)
Temperature (°C)

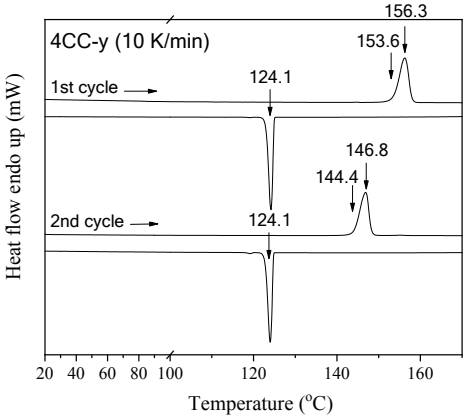
4CC-y (10 K/min)
1st cycle
2nd cycle
124.1
156.3
153.6
124.1
146.8
144.4
Heat flow endo up (mW)
Temperature (°C)

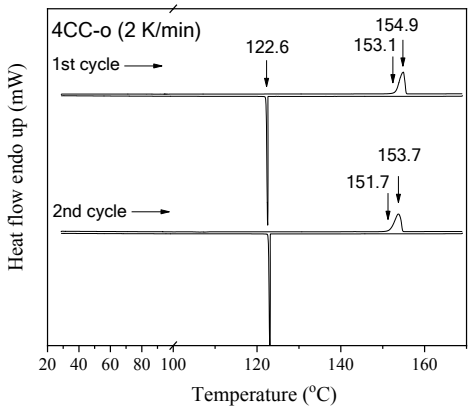
4CC-o (2 K/min)
1st cycle
2nd cycle
122.6
154.9
153.1
153.7
151.7
Heat flow endo up (mW)
Temperature (°C)

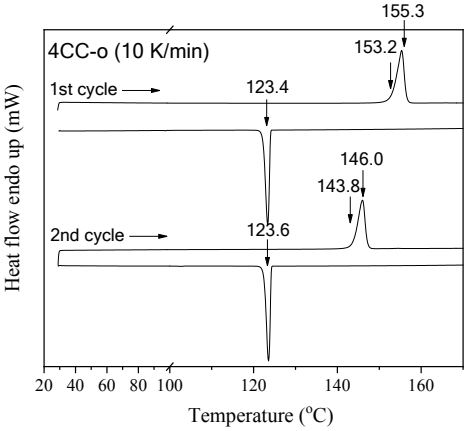
4CC-o (10 K/min)
1st cycle
2nd cycle
123.4
155.3
153.2
146.0
143.8
123.6
Heat flow endo up (mW)
Temperature (°C)

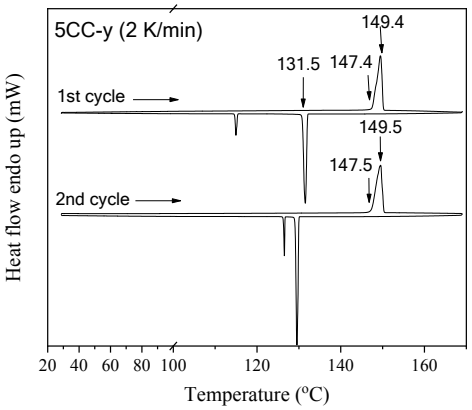
5CC-y (2 K/min)
1st cycle
2nd cycle
131.5
149.4
147.4
149.5
147.5
Heat flow endo up (mW)
Temperature (°C)

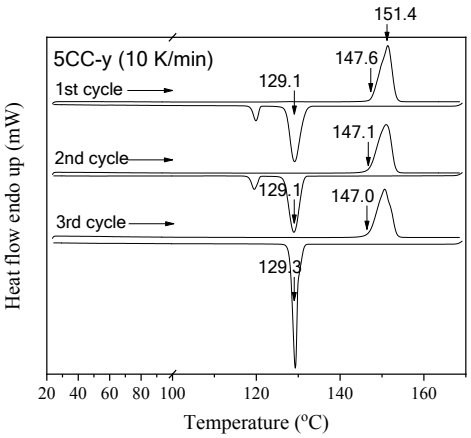
5CC-y (10 K/min)
1st cycle
2nd cycle
3rd cycle
129.1
151.4
147.6
147.1
129.1
147.0
129.3
Heat flow endo up (mW)
Temperature (°C)

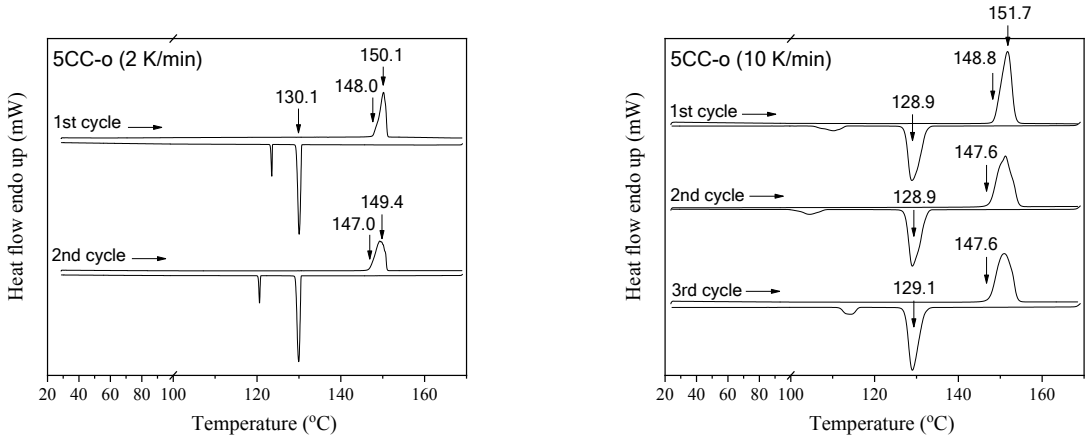

Figure S1 DSC profiles of the four crystalline samples onset and peak temperatures are indicated with arrows.

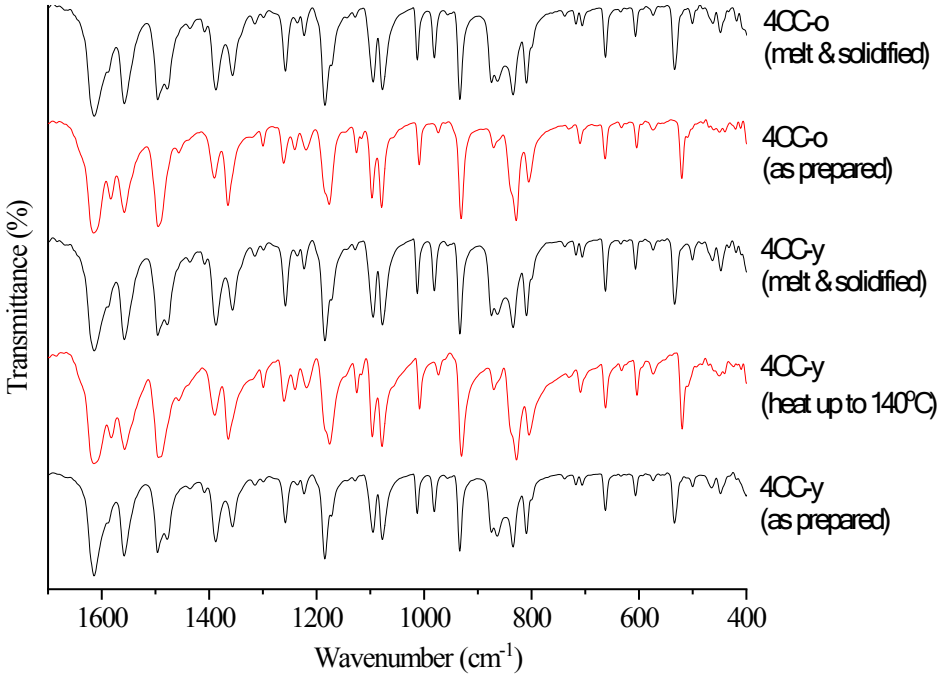

Figure S2 FT-IR spectra of 4CC-y and 4CC-o with different thermal histories. The spectra classified into the types of yellow and orange forms are shown with black and red lines, respectively.

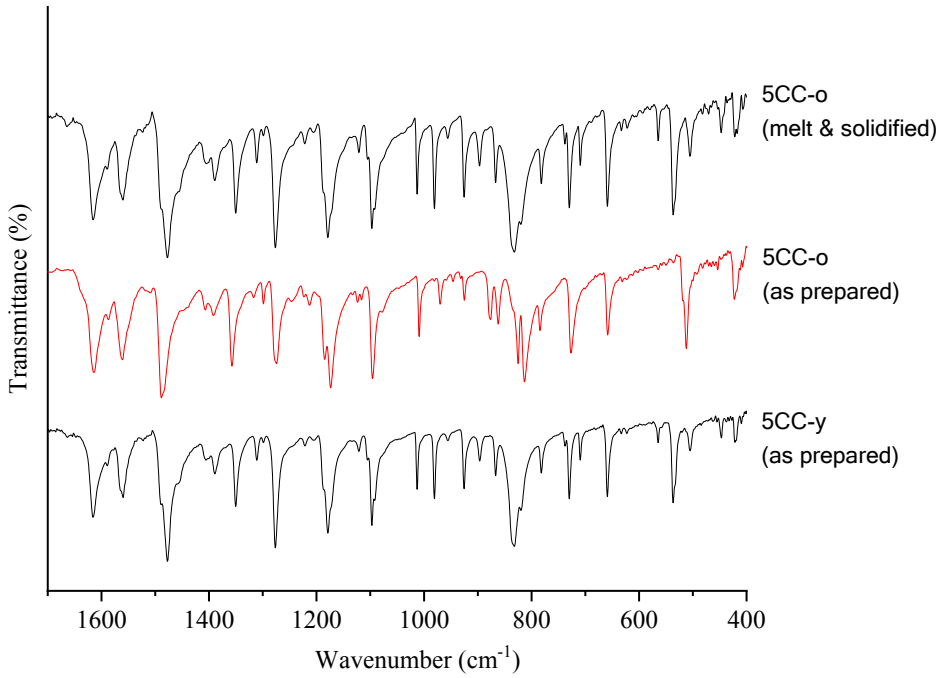

Figure S3 FT-IR spectra of 5CC-y and 5CC-o with different thermal histories. The spectra classified into the types of yellow and orange forms are shown in black and red lines, respectively.

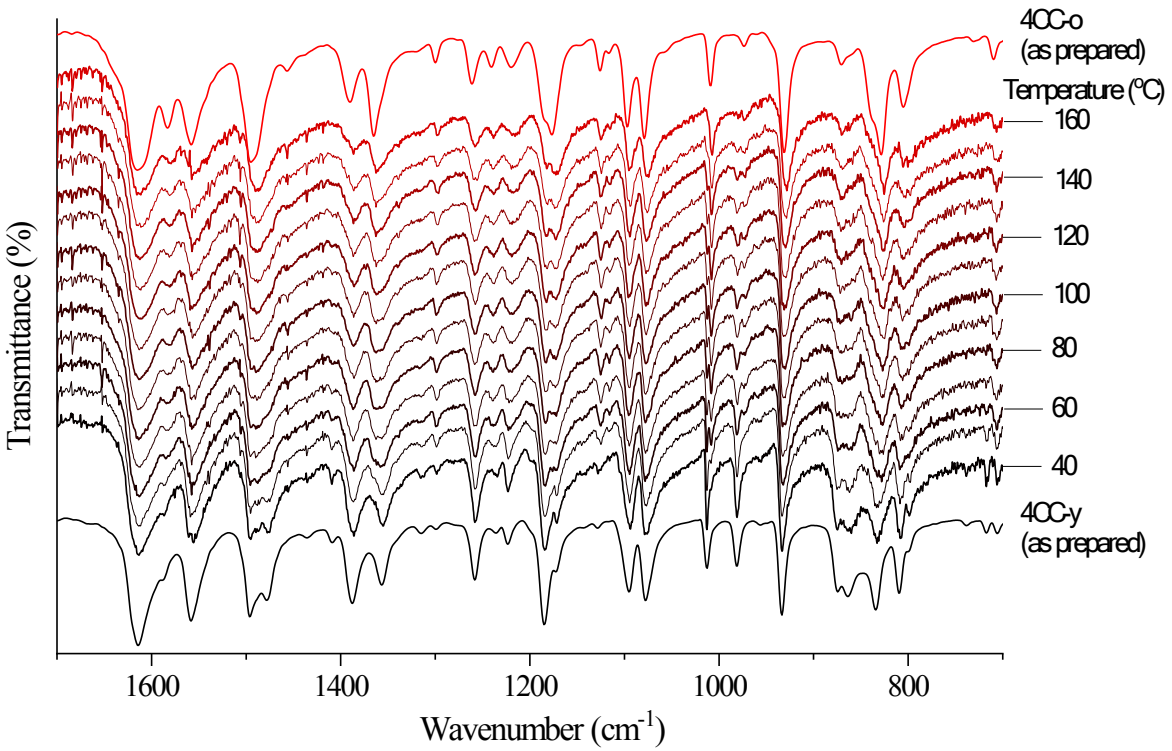

Figure S4 Variable-temperature FT-IR spectra of 4CC-y from 40 to 160 °C with an increment of 10°C. The spectra of the as-prepared samples of 4CC-y and 4CC-o are also included.

Table S3 Geometrical parameters relevant to CH…halogen and halogen…halogen interactions. Distance (d), bent angle (θ), and dihedral angle (ϕ) are as indicated in the figure below.

	d_{Cl-H}, d_{Cl-Cl} / Å	θ_{C-Cl-H}	$\theta_{C-Cl-Cl}$	$\phi_{C-Cl-Cl-C}$
4CC-y				
CH…Cl	3.065	131.8		
Cl…Cl	3.377		149.5	180.0
5CC-y				
CH…Cl (h-h)[a)]	3.001	121.8		
CH…Cl (t-t)[b)]	3.108	134.3		
Cl…Cl (h-h)[a)]	3.392		151.2	180.0
Cl…Cl (t-t)[b)]	3.393		150.8	180.0
4CC-o				
CH…Cl	2.968	132.6		
Cl…Cl	3.436		90.9, 159.6	102.0
5CC-o				
CH…Cl (h-h)[a)]	2.963	120.0		
CH…Cl (t-t)[b)]	2.997	133.9		
Cl…Cl (h-h)[a)]	3.511		114.2, 159.2	154.1
Cl…Cl (t-t)[b)]	3.463		92.6, 156.1	103.2

a) For atoms that belong to salicyl rings (head-to-head).

b) For atoms that belong to aniline rings (tail-to-tail).

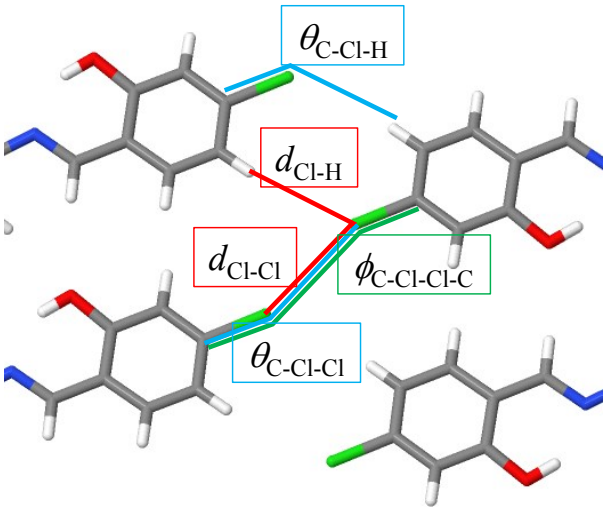

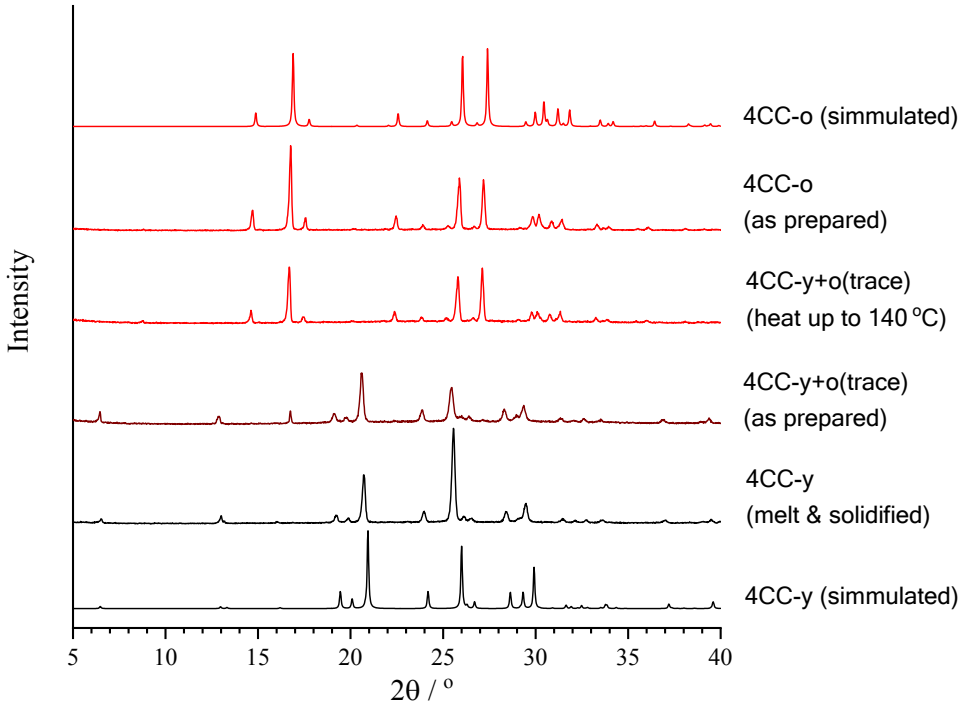

Figure S5 powder XRD patterns of 4CC-y and 4CC-o with different crystallization conditions. The patterns classified into the types of yellow and orange forms are shown with black and red lines, respectively.

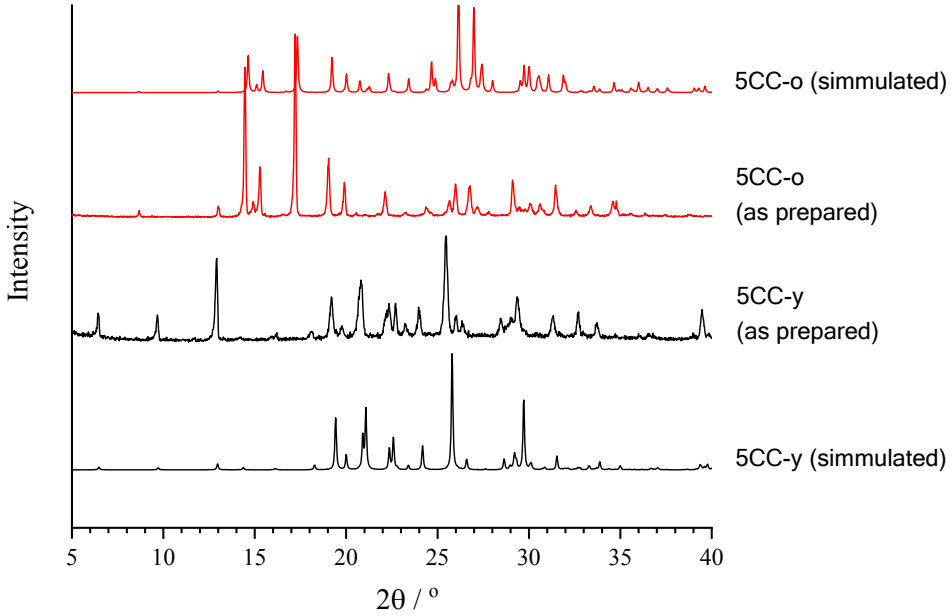

Figure S6 powder XRD patterns of 5CC-y and 5CC-o with different crystallization conditions. The patterns classified into the types of yellow and orange forms are shown with black and red lines, respectively.

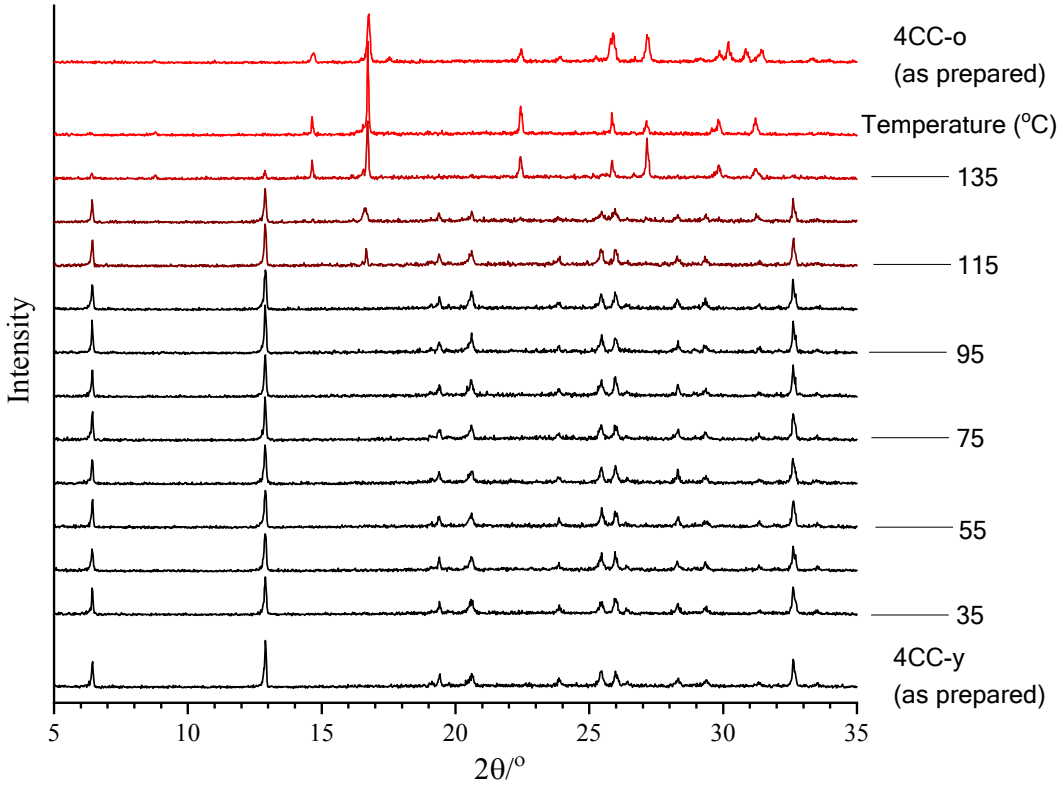

Figure S7 Variable-temperature powder XRD patterns of 4CC-y from 35 to 145 °C with an increment of 10°C. The patterns of the as-prepared samples of 4CC-y and 4CC-o are also included.

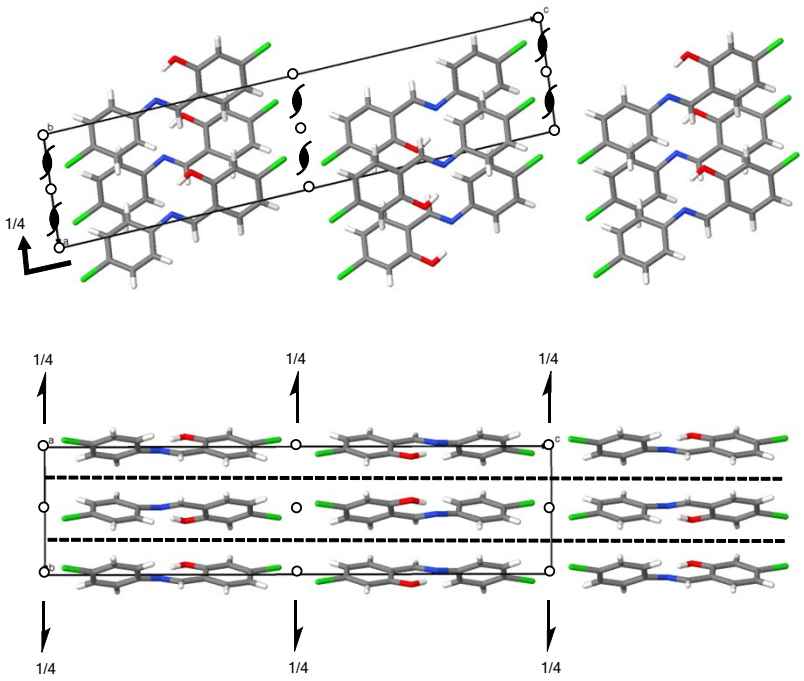

Figure S8 Molecular arrangement in a 4CC-y crystal modeled by removing the disorder and assuming $P2_1/a$ space group: viewed along the b-axis (top) and c-axis (bottom). Symbols denoting symmetry elements are overlaid.

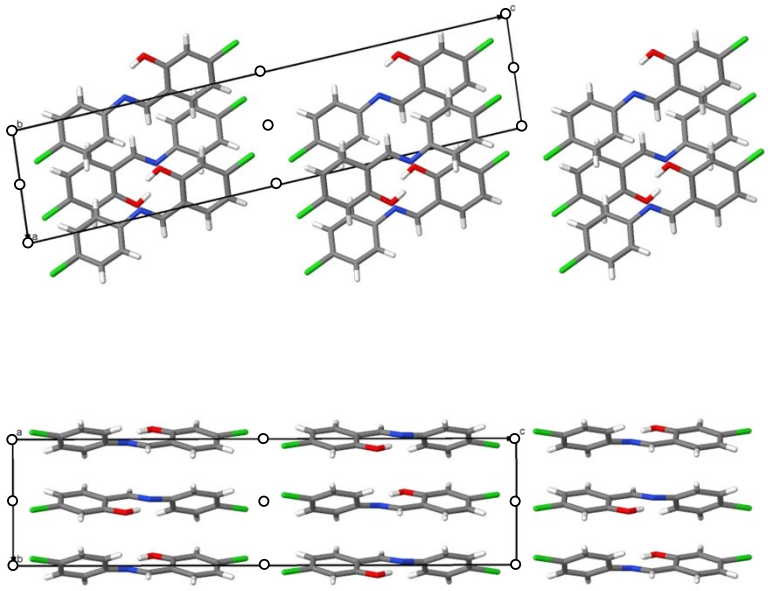

Figure S9 Molecular arrangement in a 4CC-y crystal modeled by removing the disorder and assuming *I*-1 space group: viewed along the b-axis (top) and c-axis (bottom). Symbols denoting symmetry elements are overlaid.

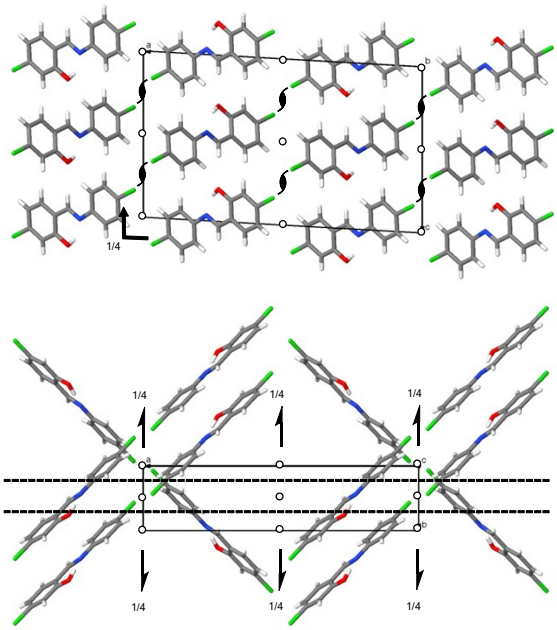

Figure S10 Molecular arrangement in a 4CC-o crystal modeled by removing the disorder and assuming $P2_1/c$ space group: viewed along the b-axis (top) and c-axis (bottom). Symbols denoting symmetry elements are overlaid.

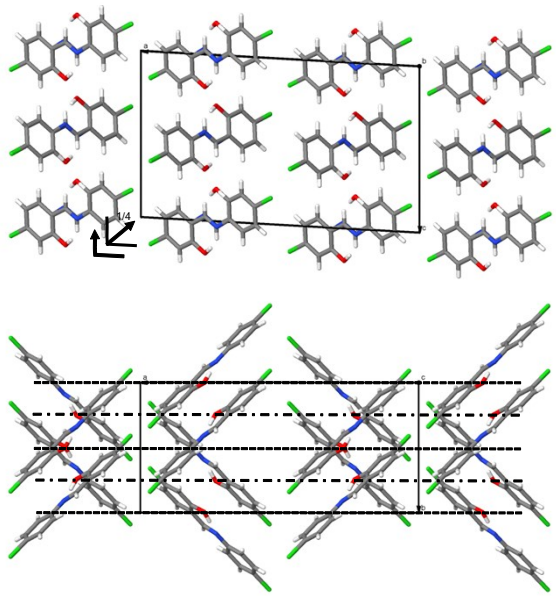

Figure S11 Molecular arrangement in a 4CC-o crystal modeled by removing the disorder and assuming *Cc* space group: viewed along the b-axis (top) and c-axis (bottom). Symbols denoting symmetry elements are overlaid.

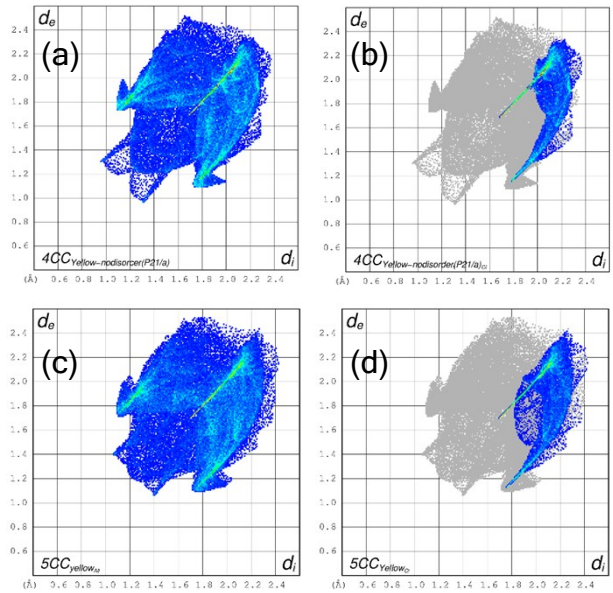

Figure S12 Crystal fingerprint plots for (a) 4CC-y ($P2_1/a$ model) and (c) 5CC-y. (b) and (d) are the partial plots contributed by Cl (interior)…any atom (exterior) pair for (a) and (c), respectively.

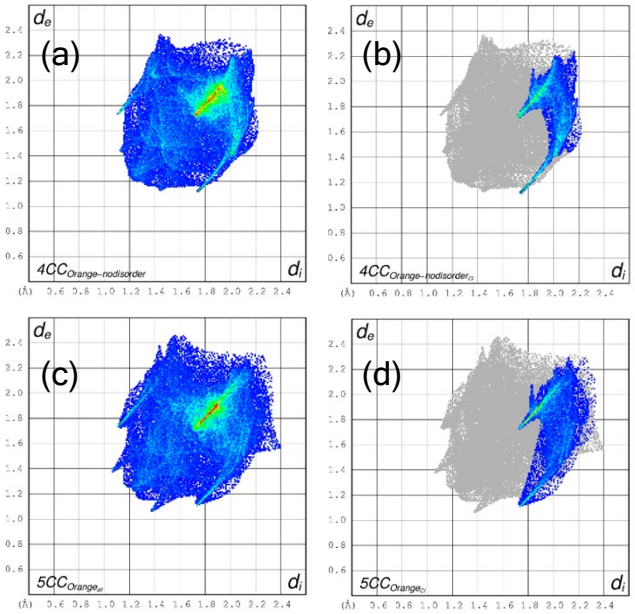

Figure S13 Crystal fingerprint plots for (a) 4CC-o ($P2_1/c$ model) and (c) 5CC-y. (b) and (d) are the partial plots contributed by Cl (interior)…any atom (exterior) pair for (a) and (c), respectively.

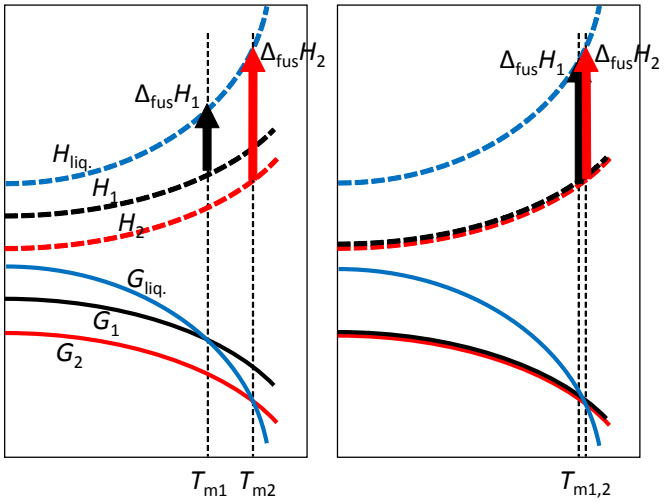

Figure S14 Schematic representation of Gibbs energy and enthalpy for 4CC (left) and 5CC (right) as functions of temperature. The quantities for yellow and orange polymorphs are denoted with subscripts 1 and 2, respectively.